Available online at www.sciencedirect.com
SCIENCE DIRECT®
ELSEVIER
International Journal of Solids and Structures 43 (2006) 435–458
INTERNATIONAL JOURNAL OF SOLIDS and STRUCTURES
www.elsevier.com/locate/ijsolstr

Stochastic modeling of multi-filament yarns: II. Random properties over the length and size effect

M. Vořechovský [a], R. Chudoba [b,*]

[a] *Institute of Structural Mechanics, Technical University Brno, Veveří 95, 602 00 Brno, Czech Republic*
[b] *Chair of Structural Statics and Dynamics, Aachen University of Technology, Mies-van-der-Rohe-Str. 1, 52056 Aachen, Germany*

Received 9 September 2004; received in revised form 23 June 2005
Available online 30 August 2005

Abstract

The present study addresses the influence of variations in material properties along the multi-filament yarn on the overall response in the tensile test. In Part I (Chudoba, Vořechovský and Konrad, 2006), we have described the applied model and studied the influence of scatter of material characteristics varying in the cross-section with no variations along the filaments. In particular, we analyzed the influence of varying cross-sectional area, filament length and delayed activation. Inclusion of these effects has lead to a better interpretation of the experimental data, especially with respect to the gradual stiffness activation, post-peak behavior and some form of size effect. In the present paper, the length-related distributions of local stiffness and strength are included in terms of theoretical considerations and by applying the Monte Carlo type simulation of random fields. Such an approach allows us (1) to demonstrate the strong need for including length scale to random fluctuation of strength along the filaments and (2) to combine several sources of randomness in a single analysis so that their significance can be evaluated from the tensile test response.

Keywords: Multi-filament yarn; Fiber bundle models; Random field simulation; Delayed activation; Size effect

1. Introduction

The present work has arisen from the need to evaluate the variations of material properties in a AR-glass multi-filament yarn used in the production of textile-reinforced concrete. The heterogeneous nature of both

* Corresponding author. Tel.: +422418050289; fax +422418022303.
E-mail addresses: vorechovsky.m@fce.vutbr.cz (M. Vořechovský), rch@lbb.rwth-aachen.de, rch@baustatik.rwth-aachen.de (R. Chudoba).

0020-7683/$ - see front matter © 2005 Elsevier Ltd. All rights reserved.
doi:10.1016/j.ijsolstr.2005.06.062

Nomenclature

A	cross-sectional area
COV	coefficient of variation
E	Young's modulus
$E[\ldots]$	mean value
$D[\ldots]$	variance
P_f	probability of failure
Q_n^*	maximum tensile force of n-filament yarn normalized by n
R_{aa}	autocorrelation function
e	yarn strain
$k_{\sigma,E}$	limiting ratio due to the spatially varying stiffness
l	nominal length of the test specimen
l_ρ	autocorrelation length
m	Weibull modulus (shape parameter)
p	number of material points used to discretize a filament in the bundle
n	number of filaments in the bundle
n_{sim}	number of simulations
s	scale parameter of Weibull distribution
G_n	cumulative distribution function of normalized yarn strength Q_n^*
$\mathscr{M}_i$	set of material points of ith filament
$f(l)$	length effect due to the spatially varying strength
$r_{\sigma,E}(l)$	length effect due to the spatially varying stiffness
μ_σ^*, μ^*	mean bundle strength for large n according to Daniels
$\mu_{\sigma,n}^*$	bundle MSEC for n according to Smith
$\mu_{\sigma,n,l}^*$	bundle MSEC with autocorrelation length for σ
$\mu_{\sigma,n,l,E}^*$	bundle MSEC with autocorrelation length for σ and E
σ	stress, strength
θ	activation strain (slack)
ξ	filament breaking strain
θ	random nature

the reinforcement and the matrix calls for thorough study of several sources of randomness that must be accounted for simultaneously.

In the preceding paper (Chudoba et al., 2006), we have analyzed the influence of variations in the filament characteristics on the total response of a multi-filament bundle in the tensile test. The study included variations in three parameters influencing the stiffness and stress evolution of a bundle during the loading in different ways: filament diameter, filament length and delayed activation of individual filaments. In spite of the differences in the form of the calculated load–strain curve, the variations in the three studied parameters have a common effect: the peak force gets reduced with a decreasing yarn length, i.e. in an opposite direction of length dependency compared to the statistical size effect in the classical sense (e.g. Weibull, 1939; Epstein, 1948; Bažant and Planas, 1998). The description of this reverse size effect is essential for the correct modeling of the bundle performance in the crack bridges occurring in cementitious composites.

Up to this point, our study of variations in the filament parameters has been focused on variations across the bundle. In the present study, we focus on the effect of the spatial distribution of the material characteristics including their autocorrelation structure, in particular the strength σ and E-modulus. In this case, we

Table 1
Material parameters identified from the yarn tensile test and used for numerical simulations

	Tensile strength, σ	E-modulus, E	Breaking strain, $\xi = \sigma/E$
Mean value	$\overline{\sigma} = 1.25$ GPa	$\overline{E} = 70$ GPa	$\overline{\xi}_{\overline{E}} = 1.786\%$
Standard deviation	0.3125 GPa	10.5 GPa	0.4464%
COV	0.25	0.15	0.25
In case of Weibull distribution (Eq. (16)) $F_X(x;s,m)$ the parameters m, s are:			
Shape parameter	$m_\sigma = 4.5422$	$m_E = 7.9069$	$m_{\xi\|\overline{E}} = 4.5422$
Scale parameter	$s_\sigma = 1.369$ GPa	$s_E = 74.373$ GPa	$s_{\xi\|\overline{E}} = 1.9557\%$

consider the randomness of the strength distribution as a stationary random process. In particular, we use a Monte Carlo type simulation method named Latin Hypercube Sampling (Iman and Conover, 1980, 1982) combined with orthogonal transformation of covariance matrix (e.g. Novák et al., 2000; Olsson and Sandberg, 2002; Vořechovský and Novák, 2003) to represent random fluctuations of filament properties. For the repeated evaluation of the randomized response we use the SFR algorithm described in Chudoba et al. (2006).

By including both cross-sectional and length-related variations in the modeling framework we are able to capture the whole loading and failure process during the test, including the size effect. An independent representation of the mentioned sources of randomness in the model allows us to focus the analysis on the separate effects in the test one after the other. Following the described calibration procedure, the influence of the considered sources of randomness on the overall response can be traced back in a systematic way.

In the paper, we first present the applied method of capturing the size effect due to the strength fluctuations along a single filament and relate the results to the local (classical) Weibull and non-local Weibull strength-based models in Section 2. After that in Section 3, we analyze the size effect due to the variations of the strength along the parallel system of filaments using both the stochastic numerical simulations and the analytical and numerical models due to Daniels's (1945), Phoenix and Taylor (1973) and Smith (1982). The effect of the randomized stiffness along the bundle is added in Section 4. Finally, in Section 5 the stochastic model is applied to the performed tests on AR-glass yarns with the demonstration of the systematic calibration procedure for identifying the material parameters and their statistical characteristics.

Consistently with Part I (Chudoba et al., 2006), we define the set of reference parameters according to Table 1. From here on, in all computations these parameters: (i) obey the appropriate PDF when considered random (ii) or are constants equal to the mean values otherwise. If all parameters are constant the bundle force T as a function of bundle strain e is directly expressed as $T(e) = M_0(e) = nEAeH(\xi - e)$, where n denotes the number of filaments, e stands for the bundle strain and $H(z)$ is the Heaviside (unit step) function; $H(z) = 1$ for $z \geqslant 0$ and zero elsewhere. The breaking strain in such a perfect bundle is 1.786%. For simplicity we assume constant filament diameter of 26 μm (circular cross-section). The material parameter values are obtained from the laboratory tests on AR-glass multifilament yarns. We emphasize that the results are not limited to this type of material.

2. Random strength along the filament

In the randomization of the material properties of the simulated yarn we distinguish the variability over the filaments $i \in \langle 1,\ldots,n\rangle$ in the yarn sections and the variability of stiffness and strength parameters over the material points of each filament $\mathscr{M}_i, j \in \langle 1,\ldots,p\rangle$. In the latter case of the spatial randomization (along the filament) it is necessary to account for distance-dependent autocorrelation of properties at two sampling points. Further, in case of strength randomization it is particularly necessary to correctly reflect the lower tail of the distribution in order to capture its minima.

In order to address these issues we analyze the correspondence between the two possible approaches to spatial randomization of the strength:

- The filament is idealized as a chain of independent random parts/sub-chains with a given length and, therefore, can be simulated by independent identically distributed (IID) random variables. This kind of spatial strength randomness corresponds with the derivation of the Weibull integral (Eq. (1)) for the failure probability P_f.
- The other possible approach is to include autocorrelation along the filament and represent randomness of material parameters by one-dimensional random field (random process). This can be supported by the argument that there must exist some distance in which the fluctuation of parameters is correlated. This distance is independent of filament length and is a constant.

Due to the direct link between the strength randomization using the IID random variables and the Weibull distribution of P_f with a known asymptotic behavior we will use it to verify the ability of the stochastic model to cover the tails of the strength distribution.

2.1. Spatial strength randomization using IID

Since we are dealing with strength of a fiber, we are interested particularly in the minima of strength realization over the filament length. It is well known from the theory of extreme values of IID that there are three and only three possible asymptotic (non-degenerate) limit distributions for minima (Fisher and Tippett, 1928) satisfying the condition $F_n(x) = [1 - (1 - F(x))^n]$. In order to avoid degeneration we look for the linear transformations with constants a_n and b_n (depending on n) such that the limit distributions $L(x) = \lim_{n\to\text{infty}} L_n(a_n x + b_n) = \lim_{n\to\infty} 1 - [1 - L_n(a_n x + b_n)]^n$. Since we are using the Weibull elemental distribution the extreme values (minima) belong to the domain of attraction of Weibull distribution, and the sequences of constants a_n and b_n satisfying the recursive relation are known (see e.g. Gnedenko, 1943; Gumbel, 1958; Castillo, 1988).

Using the weakest-link model together with the Weibull-type function for concentration of defects, the probability of failure P_f at a given level of stress σ is expressed as the so-called Weibull integral (Weibull, 1939):

$$P_f(\sigma) = 1 - \exp\left[-\int_l \left\langle \frac{\sigma}{s_0} \right\rangle^m \frac{\mathrm{d}l}{l_0}\right], \tag{1}$$

where the Malacuya brackets stand for positive part $\langle \bullet \rangle = \max(\bullet, 0)$. For a given Weibull modulus (shape parameter) m, we have a length l_0 with the corresponding scale parameter of random strength distribution s_0. In the case of a single filament, the failure stress σ is a positive constant so that we can rewrite Eq. (1) as $-\ln(1 - P_f) = l/l_0(\sigma/s_0)^m$. The strength level for a chosen level of P_f can now be expressed as a function of the filament length l:

$$\sigma(l) = s_0[-\ln(1 - P_f)]^{1/m}\left(\frac{l_0}{l}\right)^{1/m}. \tag{2}$$

This size effect equation is a power law represented as a straight line in the double-log plot of l vs. σ with the slope $-1/m$ and passing through s_0 at l_0 (see Fig. 1d). The analytical determination of the mean strength requires an integration over P_f and leads to an expression employing the Gamma function Γ:

$$\overline{\sigma}(l) = s_0\Gamma(1 + 1/m)\left(\frac{l_0}{l}\right)^{1/m}. \tag{3}$$

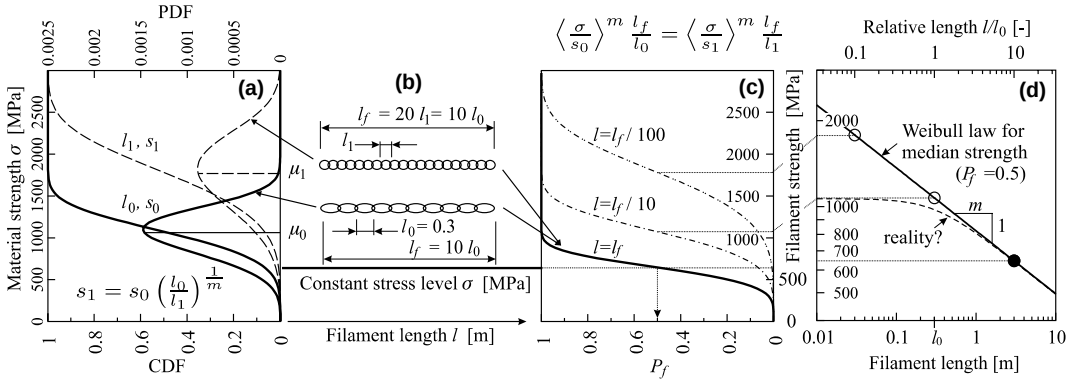

Fig. 1. Weibull scaling.

The corresponding coefficient of variation (COV) of filament strength distribution is a constant independent of the filament length given solely by the Weibull modulus m:

$$\mathrm{COV} = \sqrt{\frac{\Gamma(1+2/m)}{\Gamma^2(1+1/m)} - 1}. \tag{4}$$

Now, in order to establish the correspondence with the strength randomization by IID we visualize the important property of the Weibull distribution (Eq. (1)): the scale parameter of the Weibull distribution can be adjusted by for any length l_1 to deliver the same P_f as for the original reference length l_0:

$$\frac{s_1}{s_0} = \left(\frac{l_1}{l_0}\right)^{-1/m}. \tag{5}$$

The length l_0 is sometimes referred to as "representative" but its choice is arbitrary so that we call it "reference length" throughout the paper.

The two chains displayed in Fig. 1b have the same length l_f and different reference lengths l_0 and l_1 with corresponding scale parameters s_0 and s_1 complying with Eq. (5). Probability density function is denoted by PDF and cumulative density denoted by CDF. The diagram in Fig. 1a shows the scaled strength distributions corresponding to l_0 and l_1. For a given stress level both distributions yield the same value of P_f as shown in Fig. 1c.

As a consequence the size effect $\sigma(l)$ obtained from Eq. (2) is identical for both reference lengths l_0, l_1 and the scale parameters s_0, s_1, respectively. This can be seen on the example of the median size effect ($P_f = 0.5$) displayed in double-logarithmic plot in Fig. 1d. This demonstrates the inherent feature of the Weibull distribution in the context of the weakest-link model already revealed in Eq. (5): it is arbitrarily scalable with respect to the reference length l_0.

This feature must be kept in mind when assessing the applicability of the independent identically distributed random variable simulations. Regarding the chain segments of ith fiber in Fig. 1b as sampling points of an IID random variable simulation we may reproduce the size effect with the slope $-1/m$ from Fig. 1b numerically in the following way:

(1) assign to each segment $j \in \langle 1, p = l/l_0 \rangle$a value of random strength σ_j following the distribution in Fig. 1a,
(2) determine the filament strength by finding the minimum segment strength $\min_{j \in \mathcal{M}_i}(\sigma_j)$,

(3) repeat (1) and (2) in n_{sim} number of simulations and evaluate the mean filament strength,
(4) perform the step (3) for all the filament lengths l of interest.

Realizing that the reference length of one segment l_1 is arbitrarily scalable, we may perform this randomization with arbitrary segment length, including very small $l_1 \to 0$ with the scaling parameter $s_1 \to \infty$ and still obtain the same size effect. However, such a randomization has nothing to do with the real spatial distribution of strength along the filament. Obviously, the strength must remain bounded for short segments. Otherwise, it would be theoretically possible to measure an arbitrarily high strength with very short specimens.

This discrepancy calls for the introduction of a length scale at which the assumption of IID at the neighboring sampling points must be abandoned. The anticipated shape of the size effect law reflecting the real spatial distribution of strength for short reference lengths is plotted in Fig. 1d as a dashed line.

2.2. Spatial strength randomization using stationary random process

The length scale gets conveniently introduced in the form of an autocorrelation structure of the strength random field. From here on any applied random field will be stationary homogeneous and ergodic with autocorrelation function:

$$R_{aa}(\Delta d) = \exp\left[-\left(\frac{|\,\Delta d\,|}{l_\rho}\right)^r\right], \tag{6}$$

where l_ρ is positive parameter called *correlation length* of the random field. With decreasing distance d a stronger statistical correlation of a parameter in space is imposed. By setting the power $r = 2$ we construct the so called *squared exponential autocorrelation function* or *bell-shaped* or *Gaussian* autocorrelation function.

Advanced simulation techniques for the simulation of underlying random variables (Latin Hypercube Sampling) are coupled with an efficient implementation of orthogonal transformation of covariance matrix needed for discrete representation of random fields (vectors). Latin Hypercube Sampling method is usually used for cheap estimation of first statistical moments of response by means of simulations. This Monte Carlo type method has been tested to converge to correct results for extremes of random variables and the required number of simulations needed to capture the statistics of extremes accurately has been found, too (Vořechovský, 2004, in preparation).

A method by Vořechovský (submitted for publication) with the possibility of cross-correlated random fields has been applied to obtain material parameters reflecting the input probability distributions. For accurate generation of uncorrelated Gaussian random variables needed for the expansion of a field the optimization technique simulated annealing has been used (Vořechovský and Novák, 2002). A comparison of efficiency of different random variable simulation techniques needed for expansion of stochastic fields with a detailed error assessment has recently been published by Vořechovský and Novák (2003).

The numerical evaluation of the size effect remains the same as described in the previous section, except that the strength randomization must account for the autocorrelation. Examples of the simulated random strength field realizations are shown later in the paper in Fig. 7 for three filament lengths.

Since the most important value of the random strength process is its global minimum throughout the filament/process length, we used very dense discretization of the field. In particular, 15 discretization points were used within the autocorrelation length. Clearly, this imposes a limit for modeling of filaments, let alone yarns, because such dense grids cannot be handled by today's computers in spite of their fast development. Fortunately, such detailed modeling of minima of long process is not necessary if we know its asymptotic properties (as will be shown later).

The calculated mean size effect curve (mean minima vs. length) qualitatively follows the dashed line shown in Fig. 1d. While the right asymptote is that of the size effect obtained from the IID randomization, the left asymptote becomes constant at the level of the mean of strength distribution. This means that for very long filaments ($l \gg l_\rho$), the influence of autocorrelation between neighboring points becomes negligible and the extremes of the field become identical to extremes of IID. On the other hand, for very short filaments ($l \ll l_\rho$) the spatial fluctuations in strength become insignificant, the random strength field is replaced by a single random variable.

The transition zone between the two asymptotes is of special interest. It is an occasional practice (e.g. Bažant et al., 2005, 2004) to avoid the more expensive random field simulations by defining the mean size effect as a bilinear curve consisting of the two described asymptotes with an intersection at $[l_\rho, \mu_0]$. In such an approach the Weibull distributed IID randomization (with COV given by the Weibull modulus in Eq. (4)) is performed with the chain segments of the length l_0. Random elements larger than l_0 (considered a known material parameter) are assigned with random mean strength scaled according to Eq. (5). However, elements smaller than l_0 are assigned with the mean μ_0 being equal to the mean strength of the filament of zero length and also being the mean corresponding to the length l_0. In other words, the Weibull power law gets limited by a constant level of mean strength for elements smaller than l_0. Then, the mean strength of a filament with the length $l = l_0$ lies exactly on the intersection of the two introduced asymptotes, see Fig. 1d. While this approach gives a good approximation of the field extremes (minima) for long filaments (large structures), it obviously leads to an overestimation of the mean strength for lengths $l \approx l_\rho$ (see Fig. 4(left)). The reason is that the spatial correlation is too high and strongly influences the random strength field.

In order to introduce the statistical length scale in the Weibull power law for the size effect, we modify Eq. (2) by introducing the length-dependent function $f(l)$ as a replacement of $(l_0/l)^{(1/m)}$ in the following form:

$$\sigma(l) = s_0[-\ln(1-P_f)]^{1/m} f(l) = s(l)[-\ln(1-P_f)]^{1/m}, \tag{7}$$

where $s(l) = s_0 f(l)$, because formally we associate the length dependence of strength with the scale parameter s. By solving Eq. (7) for P_f we see that $f(l)$ affects only the scale but not the shape of Weibull strength distribution ($\mathrm{CDF} = P_f = 1 - \exp[-\sigma/(s_0 f(l))]^m$). The coefficient of variation of Weibull distribution depends on m (similarly to the Weibull IID case) and is length-independent. Therefore, it is again given by Eq. (4).

The mean size effect can be written in analogy with Eq. (3) as

$$\overline{\sigma}(l) = s_0 \Gamma(1+1/m) f(l) = s(l)\Gamma(1+1/m). \tag{8}$$

The calculated mean of minima of one Weibull random process (single filament) covering the whole range of lengths is plotted in the upper curve of the top left diagram in Fig. 4. The three introduced zones of the statistical size effect are denoted: single random variable ($l/l_\rho \to 0$), autocorrelated random field ($l/l_\rho \approx 1$) and the set of independent identically distributed random variables ($l/l_\rho \to \infty$).

We suggest to approximate the size effect obtained numerically using Eq. (7) with $f(l)$ expressed by one of the following formulae:

$$f(l) = \left(\frac{l}{l_\rho} + \frac{l_\rho}{l_\rho + l}\right)^{-1/m} \tag{9}$$

or

$$f(l) = \left(\frac{l_\rho}{l_\rho + l}\right)^{1/m}. \tag{10}$$

This approach is done intuitively by asymptotic matching (left and right asymptotes are advocated above by the reasoning; and for the transitional sizes we use a smooth "interpolation"). The numerically obtained mean of minima lies in between these two approximations. The function $f(l)$ is exploited to derive an analytical formula for combined energetic-statistical size effect of quasibrittle structures failing at crack initiation (its statistical term) in Bažant et al. (2005).

It should be mentioned, that another commonly applied way of introducing the length scale into the framework of the Weibull integral of P_f is to introduce the dependence between the sampling points of a strength randomization using IID indirectly by averaging the instantaneous stresses in the neighborhood of a material point (called non-local Weibull integral), see e.g. (Bažant and Xi, 1991; Bažant and Novák, 2000). However, in our case of a uni-axial stress state and elastic-brittle filaments, the stress level is constant along the filament so that no averaging can be performed. In our opinion, this reveals an inconsistency in combining the stress averaging and the Weibull form of the P_f in order to introduce some kind of spatial correlation. The problem is that the key concept in deriving the Weibull integral of P_f is the independency of the failure probability $P_{f,1}$ of a subelement on its neighbors (survival probabilities are multiplied), see Weibull (1939). The approach of averaging misuses the length scale introduced in phenomenological terms to mimic autocorrelation in the process zone. However, it does not necessarily reflect the statistical length scale associated with material randomness.

3. Random strength along filaments within the bundle

Having demonstrated the correspondence between the stochastic simulation and the classical Weibull theory we proceed in a similar way in the validation of the stochastic model for the bundle of n parallel filaments. Again, we shall first focus on the randomization of strength using both the random process and the simulation of independent identically distributed random variables, in order to allow for the comparison with the classical model of n parallel fibers formulated by Daniels's (1945). The comparison will be performed by means of the size effect both for the numerical (Section 3.1) and for the asymptotic analytical (Section 3.2) forms of the Daniels's model for the distribution of the normalized bundle strength $Q_n^* = \sup[T(e)/n]$.

3.1. Comparison with Daniels's numerical recursion

Daniels's (1945) considered a system of n independent parallel fibers stretched between two clamps with equal load sharing. Filaments $i \in \langle 1, \ldots, n \rangle$ share the identical distribution function of strength $F_X(x) = F_i(x) = P_i(X \leqslant x)$. Apart from the random strength all other parameters are constant. The maximum tensile force of a filament given as $Q(\theta) = X = A\sigma(\theta)$ (θ stands for random nature) gets randomized for the individual filaments: $Q_{(i)}$ and ordered ($Q_{(i)} \leqslant Q_{(i+1)}$) so that the marginal probability density function of $Q_{(i)}$ can be obtained in terms of $f_X(x)$ and $F_X(x)$ as (see e.g. Gumbel, 1958):

$$f_i(x_i) = i\binom{n}{i}[F_X(x_i)]^{i-1}[1 - F_X(x_i)]^{n-i} f_X(x_i). \tag{11}$$

The maximum tensile force of the bundle is given by

$$Q_n^* = \max_{1 \leqslant i \leqslant n}\left(Q_{(i)} \cdot \frac{n-i+1}{n}\right). \tag{12}$$

Here, the yarn load is measured in terms of load per filament, i.e. $1/n$ times the total load on the system. The distribution of Q_n^* was investigated by Daniels's (1945) under the assumption that filament strengths are

independent and identically distributed random variables with known common distribution function. Daniels's (1945) showed the distribution function of the maximum tensile force of the bundle with (IID) filaments to be:

$$G_n(x) = P\left(Q_n^* \leqslant x\right) = \sum_{i=1}^{n} (-1)^{i+1} \binom{n}{i} [F_X(x)]^i G_{n-i}\left(\frac{nx}{n-i}\right), \tag{13}$$

where $G_0(x) \equiv 1$ and $G_1(x) = F_X(x)$. The distribution functions $G_n(x)$ obtained from this recursive formula for $n = 1, 4, 8, 16$ filaments are shown as dotted curves in the top diagram of Fig. 2 for forces higher than 700 N for better legibility.

In Fig. 2, we show the results of the stochastic simulation using the IID randomization of the filament strength for the bundles with up to 800 filaments. As plotting positions of the simulations we use $i/(n_{\text{sim}} + 1)$. Both the analytical and numerical results show the gradual change of the yarn strength distribution from Weibull to asymptotically Gaussian for bundles with growing number of filaments n specified in the circle. It can be seen that the agreement between the simulation and the recursive Daniels's formula is perfect. Nevertheless, the determination of failure probabilities at the low level of stress using Monte-Carlo method requires large number of simulations. On the other hand, the recursive formula does not require any additional computational effort for small probabilities. However, as n becomes larger than 32 the recursion becomes very demanding and then the only way to estimate the probability distribution is to use stochastic simulation. In addition, the stochastic simulation combined with the SFR algorithm delivers not

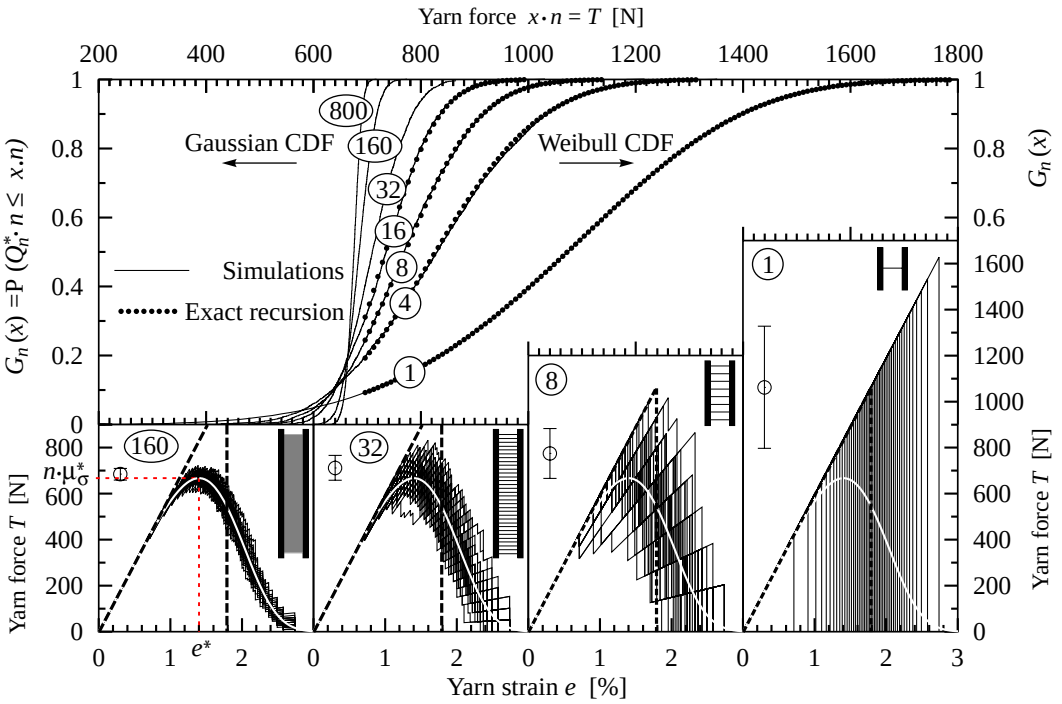

Fig. 2. Top: yarn strength distribution with growing number of filaments n obtained either using Eq. (13, for small n) or using Monte Carlo simulation. Bottom: samples of the whole force–strain diagrams obtained by the SFR algorithm for selected n in the yarn. Yarns are sketched and the mean value of strength ± standard deviation is marked by a circle with errorbars. White line shows the asymptotic mean force–strain diagram $M(e)$ (Eq. (15)).

only the strength distribution but is also able to trace the whole loading process as shown in the three diagrams at the bottom of Fig. 2.

3.2. Comparison with available asymptotic results

For the verification of the asymptotic convergence of stochastic simulation with independent identically distributed random filament strength we shall exploit the fact that for $n \to \infty$ the distribution function $G_n(x)$ converges to normal distribution (Daniels's, 1945). In particular, Daniels obtained positive constants μ_σ^* and γ_σ^* such that $\sqrt{n}(Q_n^* - \mu_\sigma^*)/\gamma_\sigma^*$ tends to a normal random variable with zero mean and unit standard deviation. In other words, for large n the distribution function of the normalized bundle strength, $G_n(x)$ can be approximated as

$$G_n(x) = P\left(Q_n^* \leqslant x\right) \approx \Phi\left(\frac{x - \mu_\sigma^*}{\gamma_\sigma^*}\sqrt{n}\right), \tag{14}$$

where $\Phi(\cdot)$ stands for standard normal cumulative density. The parameters of distribution (the mean value and variance of the bundle strength) are: $\mu_\sigma^* = E[Q_n^*] = x^*[1 - F(x^*)]$, $\left(\gamma_\sigma^*\right)^2/n = D[Q_n^*] = (x^*)^2 F(x^*)[1 - F(x^*)]$. The result is valid under the conditions that the value x^* maximizing the function $\mu(x) = x[1 - F(x)]$ is unique and positive and $\lim_{x\to\infty}\mu(x) = 0$, so $\mu_\sigma^* = \mu(x^*) = \sup[\mu(x)],\ x \geqslant 0$ and for unit yarn stiffness. We remark that some authors use the symbols μ^* and σ^* for μ_σ^* and γ_σ^*, respectively.

By reformulating the problem in random breaking strain ξ rather than filament strength as done by Phoenix and Taylor (1973) the Daniels's result can be interpreted in more transparent fashion. With E-modulus constant, the distribution of breaking strain is obtained by dividing the random strength by $\overline{E}$, see the last column in Table 2, $s_\sigma = \overline{E}s_\xi$, $m_\sigma = m_\xi$. In this case the function $\mu(e) = \mu_\sigma(e) = \mu_\xi(e)$ represents the normalized asymptotic mean yarn load–strain function for $n \to \infty$ and reads (a derivation misprinted in (Daniels, 1989)):

$$\mu_\xi(e) = \int_0^\infty q(e,\xi)\,\mathrm{d}F_\xi(\xi) = EAe\int_0^\infty H(\xi - x)\,\mathrm{d}F_\xi(\xi) = EAe\int_{\xi=x}^\infty f_\xi(\xi)\,\mathrm{d}\xi = EAe[1 - F_\xi(e)], \tag{15}$$

where $q(e,\xi)$ is the constitutive law of a filament (see Part I) and $F_\xi(e)$ $[f_\xi(e)]$ is the CDF [PDF] of filament breaking strain, respectively. As noted later by Daniels (1989) such formulation in strains is more flexible and allows one to prove the asymptotic normality of peak load $\sup[u(e)]$ under more relaxed conditions (e.g. random elastic modulus, see later).

Table 2
Influence of randomness in material parameters on the measured load–strain diagrams with increasing length

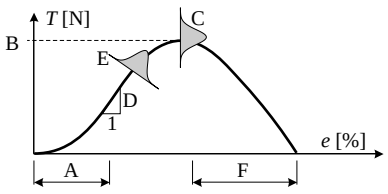

	Fixed distributions				
	$l_{\lambda_{(i)}}$	$A_{(i)}$	$l_{\theta_{(i)}}$	m, s_ξ, $f(l)$	$E_{(i),j}$
$A(l)$: evolution of initial stiffness	(·)	(·)	(−)	(·)	(·)
$B(l)$: mean peak load	(+)	(·)	(+)	(−)	(+)
$C(l)$: scatter of peak load	(·)	(·)	(−)	(−)	(−)
$D(l)$: mean stiffness	(+)	(·)	(+)	(·)	(·)
$E(l)$: scatter of stiffness	(−)	(·)	(−)	(·)	(−)
$F(l)$: post-peak range	(−)	(·)	(−)	(−)	(−)

If we consider Weibull distribution (with s and m representing the scale and shape parameters, respectively)

$$F_X(x;s,m) = 1 - \exp\left[-(x/s)^m\right] \tag{16}$$

to be a distribution of random filament strength (with parameters $s = s_\sigma$, $m = m_\sigma = m_\xi$); the parameters of asymptotically normal yarn strength can be easily obtained in terms of forces as

$$\begin{aligned} x^* &= A \cdot s_\sigma \cdot m^{-1/m} = EAe^*, \\ \mu^*_\sigma &= x^* \cdot c, \\ \gamma^*_\sigma &= x^* \cdot \sqrt{c(1-c)}, \quad c = \exp(-1/m). \end{aligned} \tag{17}$$

In this case the result of asymptotic normality of strength Q^*_n is valid in the central region of the distribution. Clearly, if the strength of filaments is Weibull (limited from left by a zero threshold) the tail of Q^*_n cannot become Gaussian (Q^*_n must have a Weibull tail). However, the distance from the mean value (central part) to the tail measured in the number of standard deviations gets so large with high n that the tail gets practically unimportant.

Taking a closer look at the asymptote one can observe slowness of convergence (as $n^{-1/6}$). It should be pointed out that $G_n(x)$ is quite straight on normal probability papers even for small n so in that respect the approximation is good. Also the variance of numerically obtained $G_n(x)$ is very close to that predicted by Daniels's result. However, the error in mean value (shift) disappears extremely slowly with growing n. The reason is that for small number of filaments n the maximum Q^*_n can be reached at wide range of e, not just e^*. As $n \to \infty$ the action point e shrinks from the wide range to e^* only.

Smith (1982) found a way to eliminate the gap between the real $G_n(x)$ and Daniels's normal approximation by adjusting μ^*_σ to $\mu^*_{\sigma,n}$ using the actual (finite) number of filaments n in the following way:

$$\mu^*_{\sigma,n} = \mu^*_\sigma + n^{-2/3} b^* \lambda. \tag{18}$$

For full derivation, see Smith (1982). In case of Weibull $F_X(x)$ the parameter $b^* = s_\sigma \cdot m^{-(1/m+1/3)} \exp[-1/(3m)]$ and the coefficient $\lambda = 0.996$. The error of approximation is then at most $O(n^{-1/3}(\log n)^2)$ which is an excellent improvement, mainly for small numbers of filaments in the bundle. For $n \to \infty$ the Smith's prediction $\mu^*_{\sigma,n}$ converges to Daniels's μ^*_σ.

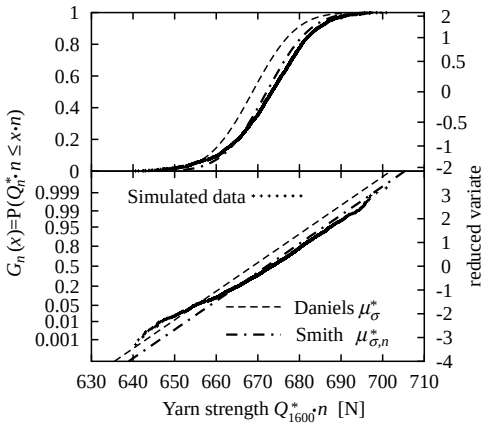

Fig. 3. Comparison of simulated data, Daniels's and Smith's normal approximation for a yarn with $n = 1600$ filaments with independent identically distributed random strength in linear plot and normal probability paper.

In accordance with Part I, the bundle strength corresponding to normalized forces $\mu^*_\sigma \mu^*_{\sigma,n}$) is given as $M^*_\sigma = n\mu^*_\sigma$ ($M^*_{\sigma,n} = n\mu^*_{\sigma,n}$, respectively). The strength randomization of 1600 filaments by IID is displayed both in the linear plot and normal probability paper in Fig. 3 and its best fit by a Gaussian distribution is compared to Daniels's and Smith's analytical results, respectively. In our case the Weibull modulus is $m \doteq 4.54$ (see Table 1), value typical for glass or polymer fibers ($\mathrm{COV}_\sigma = 0.25$). For the example of a yarn with $n = 1600$ filaments the mean value of normal approximation of maximum bundle force predicted by Daniels's is $M^*_\sigma = 668.7$ N and Smith's refined value is $M^*_{\sigma,n} = 672.1$ N. Our numerical simulation by Monte Carlo delivers the average bundle strength 672.7 N so the Smith's refinement is an excellent performer. The standard deviation of the yarn strength is numerically estimated to be equal to 9.674 N and Daniels's formula provides $\gamma^*_\sigma \cdot \sqrt{n} = 8.297$ N. For the sake of comparison, plots of Daniels's approximation, Smiths's refinement and the Monte Carlo simulations on a probability paper are plotted in Fig. 3. The analytical formula due to Daniels's (1945) results in mean strength shifted far from the exact one for small bundles.

3.3. Size effect of bundles for variable number of filaments n

In the stochastic simulations, we used the response tracing algorithm based on the superposition of the filament response (SFR) described in the previous paper by Chudoba et al. (2006) together with simulation of random process needed for spatial randomization of strength. From here on we will use the abbreviation MSEC for mean size effect curve (a curve in the bi-logarithmic plot of size vs. mean bundle strength). In Fig. 4(left) we have plotted the MSEC for various numbers of filaments in the randomized bundle. The right scale in Fig. 4(left) shows the efficiency of the bundle depending on the number of filaments n and the yarn length l. It looks like the parallel curves are only shifted downwards with increasing n. The intersection of the horizontal asymptote with the inclined IID asymptote seems to happen always at the autocorrelation length l_ρ that propagates unchanged to bundles with growing n. This is an important property because it indicates that the size effect can be expressed as a product of the length effect and of the effect of increasing n. In order to document this we formulate the bundle strength depending on its length in analogy

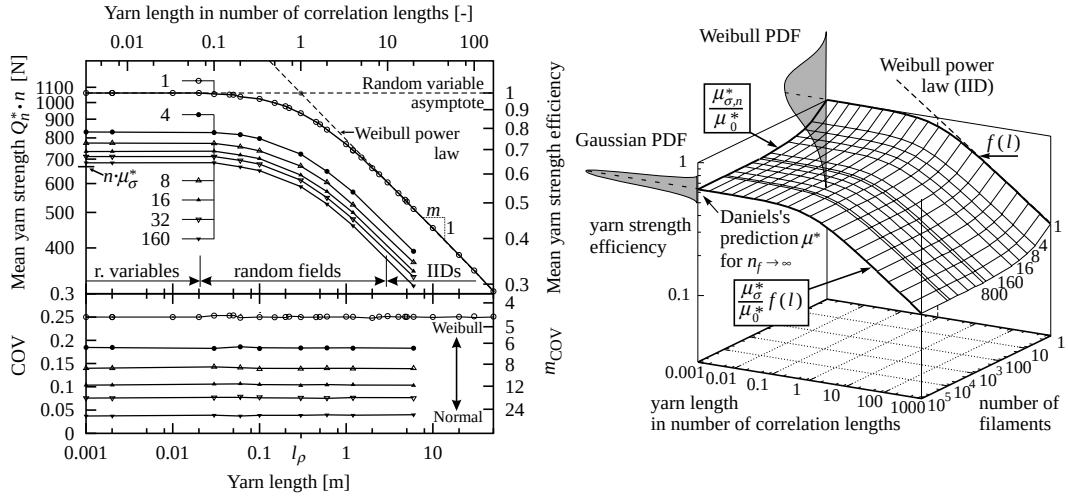

Fig. 4. Left top: mean size effect curves (MSEC) for increasing number of filaments n in a bundle for filament strength described by Weibull random process. Curves nearly overlap for n higher than 160. Left bottom: effective Weibull modulus m, Eq. (4). Right: 3D representation of yarn efficiency depending on the number of filaments and yarn length for the case of random strength described by random processes.

with Eq. (7) by associating the length dependence of breaking strength with the scale parameter $s_\xi(l) = s_\xi \cdot f(l)$ in the Weibull distribution $F_\xi(e; s_\xi(l), m_\xi)$ given in Eq. (16). After substituting this length-dependent distribution into Eq. (15) we obtain the mean load–strain diagram:

$$\mu_\xi(e,l) = EAe \exp\left[-\left(\frac{e}{s_\xi f(l)}\right)^m\right]. \tag{19}$$

The asymptotic mean peak load $\mu^*_\xi(l)$ is attained at the stationary point e^*:

$$\frac{\mathrm{d}\mu_\xi(e,l)}{\mathrm{d}e} = 0 \rightarrow e^*(l) = [f(l)m]^{-1/m} s_\xi.$$

Substituting the strain e^* into Eq. (19) we obtain the mean size effect of the bundle strength (compare with Eq. (17)):

$$\mu^*_\xi(l) = \mu_\xi(e^*, l) = EA \cdot m^{-1/m} s_\xi \exp(-1/m) \cdot f(l) = \mu^*_\sigma f(l). \tag{20}$$

Indeed, with regard to the Daniels's assumption of common strength distribution of independent filaments that applies for any length we may express the normalized and total Weibull bundle strength in dependence on l and n using Eq. (18) as

$$\mu^*_{\sigma,n,l} = \mu^*_{\sigma,n} \cdot f(l); \quad M^*_{\sigma,n,l} = \mu^*_{\sigma,n,l} \cdot n. \tag{21}$$

In other words both effects can be evaluated independently using either analytical formulation or stochastic SFR simulation. Subsequently, they can be composed using Eq. (21) into a combined size effect surface. An example of such a surface constructed with $f(l)$ given in Eq. (10) and with mean bundle strength $M^*_{\sigma,n}$ calculated numerically with the SFR algorithm is plotted in Fig. 4 right. Obviously, with $n \rightarrow \infty$ the surface Eq. (21) reduces to the curve $M^*_\sigma f(l)$. This demonstrates that the mean strength is asymptotically independent of the number of filaments n.

Regarding the strength variability of the yarn we note that COV of strength depends on Weibull modulus m irrespective the length. Fig. 4(left) bottom presents effective values of the Weibull modulus m_{COV} computed for different numbers of filaments from COV by solving Eq. (4). Of course, only for the case of a single-filament-bundle the value m_{COV} really represents a shape parameter of Weibull strength distribution. On the other hand, COV decreases for growing n with the rate $1/\sqrt{n}$. To summarize, while the weakest-link model (series coupling and extending in length) leads to the decrease of mean and constant COV, the yarn (parallel coupling and increasing n) results in asymptotically constant mean and fast decay of COV.

With the two first statistical moments available it remains to comment on the distribution of the strength. In case of a single filament, the PDF of Q^*_1 remains Weibull. With increasing n the probability distribution of Q^*_n gradually changes to Gaussian (Daniels's, 1945), see Fig. 4(right).

4. Interaction of random stiffness and strength along the bundle

4.1. Random E-modulus and strength along a single filament

Spatial fluctuation of $E(\chi)$ along a single filament is considered as autocorrelated random process. Its effect can be included in the numerical model described in Part I using equidistant discretization of ith filament with p number of points. The effective E-modulus is obtained by static condensation as (see Fig. 6)

$$E_{(i)} = p\left(\sum_{j=1}^{p} E^{-1}_{(i),j}\right)^{-1}. \tag{22}$$

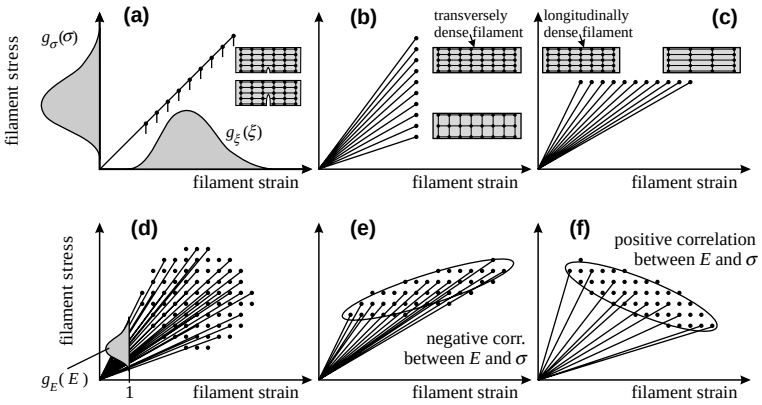

Fig. 5. Randomized constitutive law of filaments. First row: one-parameter randomization: (a) constant E, (b) constant ξ, (c) constant σ. Second row: two-parameter randomization by E and σ: (d) uncorrelated, (e) negatively correlated and (f) positively correlated.

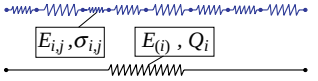

Fig. 6. Effective material stiffness $E_{(i)}$ and filament strength as a minimum strength over the filament length $Q_i = \min_j(A\sigma)_{i,j}$. Area $A_{i,j} = \text{const.}$ in present study.

We notice that the fluctuations get smeared for long filaments ($l/l_\rho \to \infty$) and the effective material stiffness converges to its limiting value E_∞. In other words, the scatter $E_{(i)}$ vanishes for very long filaments. For very short filaments $l \ll l_\rho$ the effect of scatter might be significant because $E(\chi)$ is constant along the filament and the random process reduces to a random variable $E_{(i)}$ with the distribution $G_E(E)$. The evolution of the random variable $E_{(i)}$ over the length is automatically captured by the transformation given in Eq. (22).

The variations of E-modulus cannot be considered independently of the failure threshold of a filament. The parameters E, σ and ξ are interrelated through the constitutive law. By keeping these parameters constant one at a time we can visualize three types of dependencies between them as shown in the first row of Fig. 5. These cases are examples of one-parameter randomization of the constitutive law. The case of constant E shown in Fig. 5a with linear transformation between random strength σ and breaking strain ξ has been considered in modeling the scatter of strength in Sections 2 and 3. Two other special cases with constant ξ and σ are shown in Fig. 5b and c, respectively. In order to connect the considered cases to a physical interpretation of reality we add grids of idealized material structure illustrating the source variations rendering the displayed effects. Here we assume that an increase of grid density in transversal direction increases the cross-sectional strength and increase of grid density in any direction increases the material stiffness. For completeness, the case depicted in Fig. 5a is illustrated by interrupted bindings (flaws) in the material grid not affecting the material stiffness. The asymptotic behavior of these three cases is elaborated further in Section 4.2.

In order to be able to simulate real material behavior we have to abandon the assumption of a constant parameter and assume two random inputs, possibly correlated (two-parameter randomization). Examples of uncorrelated, negatively correlated and positively correlated E-modulus and σ are shown in Fig. 5d–f. Unfortunately, there is no sound basis for choosing any kind of this correlation. The dependency between E-modulus and strength stems from variations in the micro-structure of the material that are generally unknown. Therefore, in the study of their simultaneous effect in Section 4.3 we shall stick to the general case of two uncorrelated random variables or processes.

4.2. One-parameter randomization of the constitutive law along the bundle

The numerical study using the randomized E-modulus in the bundle has been performed with n-variate uncorrelated 1D fields (processes). For comparison an isolated strength randomization has been performed as well. The parameters of applied normal distributions of randomized E-modulus and σ are summarized in Table 1. The spatial randomization has been performed with common squared-exponential autocorrelation function (Eq. (6)) both for E-modulus and for strength σ.

Similarly to Part I the yarn performance is illustrated qualitatively using the load–strain diagram on a yarn with 16 filaments only. The real number of filaments in the yarn is approximately 100-times higher. In order to have the resulting forces in the figures comparable to the real values, the forces are given in cN. Of course, the true maximum force of 1600 filament bundle cannot be obtained by scaling up the results from the small bundle. Nevertheless, the small bundle can be effectively used to study the effects of random stiffness, strength and their interactions with varying length. The simulation of real yarns is post-poned to Section 5.2.

In particular, randomness of either E or σ was simulated as 16-variate Gaussian random process (16 uncorrelated random processes) discretized using vectors with p number of material points $j \in \mathscr{M}_i$ for each filament $i = 1, \ldots, 16$. The simulated random process for three ratios between the nominal length and the autocorrelation length l/l_ρ is shown in the first row of Fig. 7. The left scale in the first row shows values of the tensile strength σ while the scale on the right presents values of the E-modulus. The sample of

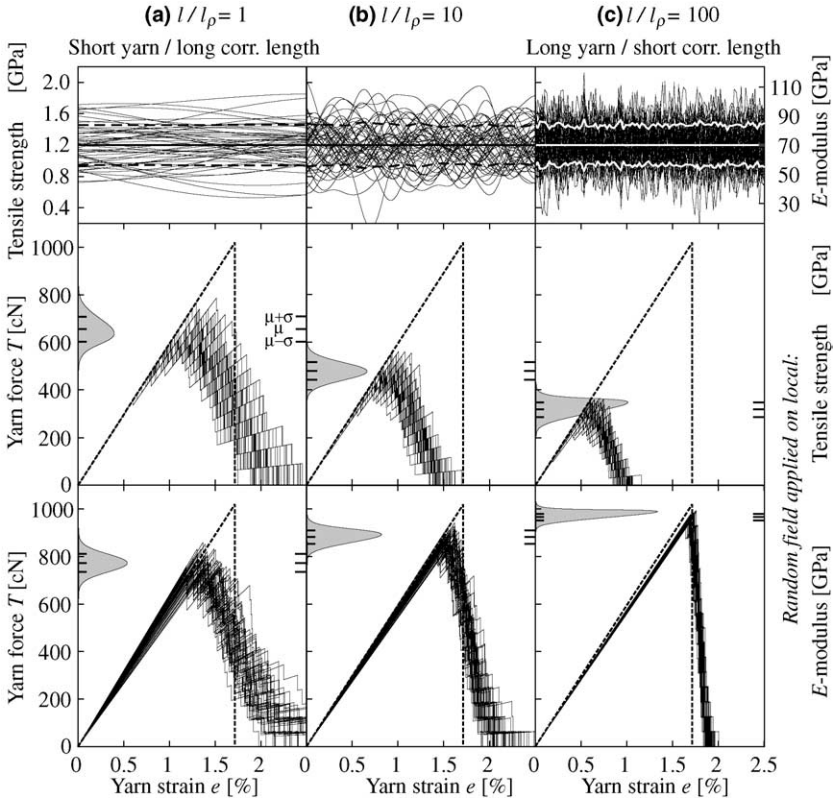

Fig. 7. Comparison of the three random fields with different correlation lengths and load deflection diagrams of 16 filament yarn with fields applied to σ and E.

$n_{\text{sim}} = 50$ realizations of the random field is plotted representing the properties of one filament in a bundle of 16 (filaments). Due to the identical autocorrelation structure the realizations of E and σ are qualitatively similar. The performed 50 bundle realizations might not be sufficient for reliable estimation of statistics, especially when higher statistical moments of the response (or even reliability) are targeted. We must keep in mind that n_{sim} must be significantly increased to ensure that the samples represent high-dimensional space of independent Gaussian random variables needed for expansion of the fields in case of long specimens ($l/l_\rho \to \infty$). Besides the calculated load–strain curves for random strength σ and E-modulus, Fig. 7 shows the mean value and standard deviation of the resulting peak force together with the sketch of the corresponding PDF.

The results obtained with the randomized strength are shown in the second row of Fig. 7 and demonstrate once again the reduction of maximum tensile force with an increasing nominal length l. Except of the reduction of the maximum load we observe the reduced scatter of the response for short specimens which is a classical feature of the statistical size effect. With regard to the previous studies of size effect due to random strength we note that the three chosen ratios $l/l_\rho \in \langle 1, 100\rangle$ (the first row in Fig. 7) fall into the transition zone between the random variable case and the IID case for each filament discussed in Section 2.2 (see Fig. 4).

The effect of fluctuating E-modulus is shown in the third row of Fig. 7. The response curves reveal a scatter of stiffness that gets (i) amplified for short yarns (or larger autocorrelation lengths) and (ii) vanishes for long yarns (see Section 4.1). Regarding the bundle strength we observe the opposite size effect because short filaments do not attain their peak load simultaneously.

In order to capture the maximum effect of variation in stiffness occurring for $l/l_\rho \to 0$ on bundle strength we study the case of $E_{i,j} = E_{(i)}$ both analytically and numerically. The variability of $E_{(i)}$ is given by the PDF $g_E(E)$ or the CDF $G_E(E)$. The asymptotic mean load–strain diagram is plotted for (a) constant filament strength $\overline{\sigma}$ or (b) constant breaking strain $\overline{\xi}$. These two cases are illustrated in Fig. 8 using 16 filaments in a yarn and Weibull distributed E-modulus with parameters specified in Table 1. For comparison we plot the asymptotic mean load–strain diagram for n infinite following the approach of Phoenix and Taylor (1973), see Section 3.2 in Part I. The diagram is generally computed as $\mu_E(e) = \int_0^\infty q(e)\,\mathrm{d}G_E(E)$. In case (a) in Fig. 8a (corresponding to Fig. 5c) the mean response reads

$$\mu_{E|\overline{\sigma}}(e) = Ae \int_0^\infty EH(\overline{\sigma}/E - e)\,\mathrm{d}G_E(E).$$

In case (b) (corresponding to Fig. 5b) the mean diagram equals to $\mu_0(e)$, a response of a perfect yarn with mean properties:

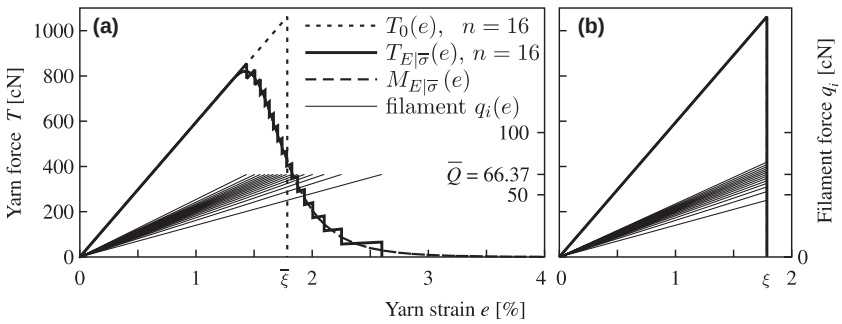

Fig. 8. Filament and yarn response in case of Weibull distributed E-modulus. Comparison of case with 16 filament yarn and asymptotic behavior with $n \to \infty$. The filaments' diagrams are plotted with respective forces on the right scale. Left: case with constant filament strength. Right: case with constant breaking strain.

$$\mu_{E|\overline{\xi}}(e) = AeH\left(\overline{\xi} - e\right) \int_0^\infty E \,\mathrm{d}G_E(E) = \overline{E}AeH\left(\overline{\xi} - e\right).$$

This case is equivalent to the random A studied in Part I.

4.3. Two-parameter randomization of the constitutive law along the bundle

In order to describe the size effect of real bundles in its complexity we consider the randomness of strength (or breaking strain) and E-modulus simultaneously. As concluded in Section 4.1 the random fields of E and σ along each filament are uncorrelated and filaments are independent. The asymptotic behavior for $l \to 0$ and $l \to \infty$ can be expressed analytically provided $n \to \infty$.

In particular, the mean load–strain diagram of very short bundles can be solved for both E-modulus and strength σ considered as random variables with distributions $G_E(E)$ and $G_\sigma(\sigma)$:

$$\mu_{\sigma,E}(e) = \int_0^\infty \int_0^\infty q(e,\sigma,E)\,\mathrm{d}G_E(E)\,\mathrm{d}G_\sigma(\sigma) = Ae \int_0^\infty \int_0^\infty H\left(\frac{\sigma}{E} - e\right) E \,\mathrm{d}G_E(E)\mathrm{d}G_\sigma(\sigma). \tag{23}$$

Unfortunately, this expression features ratio of two random variables and cannot be generally simplified. For very long bundles we get rid of this ratio by realizing that E-modulus gets homogenized over the filament length so that the random strength can be transformed to random breaking strain ξ (see Fig. 5a). The corresponding mean load–strain diagram is identical to that in Eq. (15). In case of Weibull distribution of random breaking strain: $G_\xi(\xi) = F_X(\xi; s_\xi, m_\xi)$, $\xi = \sigma/E_\infty$, we can write $\mu_{\xi,E}(e) = AE_\infty e \exp[-(e/s_\xi)]^{m_\xi}$.

In a similar way, it would be possible obtain the covariance of any pair of strains e_i, e_j (Phoenix and Taylor, 1973). With the known mean value and variance of the bundle strength evaluated at e^* we actually know the whole distribution function. This conclusion results from the following arguments.

The original Daniels's proof of asymptotic normality of bundle strength distribution has been derived under the assumption of equal (deterministic) stiffness. In the strain-based setting (Phoenix and Taylor, 1973) the asymptotic normality has been demonstrated by Phoenix (1974, 1975, 1979) under less strict assumptions than those used by Daniels's (1945). Later Daniels's (1945) elaborated more on the asymptotic distribution of strength using his former results on extremes of Gaussian processes. Also Hohenbichler (1983) has shown that the asymptotic normality is valid under certain weak dependencies between filament strengths and for independent filaments but with general force–displacement relations. Based on the procedure of Hohenbichler and Rackwitz (1983) the exact distribution can be determined from the system reliability results. The procedure is based on the transformation of two pairs of input random variables (filament strength σ and a corresponding breaking strain) into standardized space of uncorrelated normal variables and computed the reliability using first order reliability method (FORM). Even though the asymptotic distribution is known for many cases, this result is not always a good approximation for small to medium-size yarns (in terms of n). This is because the convergence to the asymptotic distribution is very slow. For general description of the size effect we employ the numerical approach.

Having described the asymptotic cases we propose to bridge the transition between short and long yarns. We want to express the mean size effect curve in the form

$$\mu^*_{\sigma,E,n,l} = \mu^*_{\sigma,n} \cdot f(l) \cdot r_{\sigma,E}(l), \tag{24}$$

where $r_{\sigma,E}(l)$ approximates the relative strength reduction due to the simultaneous scatter of E and σ. For this purpose we suggest the approximation of relative strength reduction in the form

$$r_{\sigma,E}(l) = k_{\sigma,E}\left(1 + \frac{l_\rho}{\frac{1}{7} + L_p}\right), \quad L_p = l_\rho \frac{k_\sigma, E}{1 - k_{\sigma,E}}, \tag{25}$$

where $k_{\sigma,E}$ is the ratio between the bundle strength of short yarn ($l \ll l_\rho$) with (i) both E and σ random and (ii) random σ:

$$k_{\sigma,E} = \lim_{l\to 0} \frac{\mu^*_{\sigma,E}(l)}{\mu^*_{\sigma}(l)}. \tag{26}$$

We note that the left and right asymptotes of $r_{\sigma,E}(l)$ are horizontal and, thus, preserves the asymptotic properties of the MSEC due to the scatter of strength discussed in Section 3.

As a final remark we add that the discussed effects should generally be considered in interaction with the scatter of delayed activation θ and of the relative distance of clamps λ occurring and thoroughly studied in Part I. This would be true if the autocorrelation length is shorter than the effective filament length. This means that in the case of a crack bridge the autocorrelation length would have to be of order of millimeters or less. As will be shown in the next section, this is not the case for the tested yarns so that this kind of interaction can be disregarded.

5. Application to the experiment

Putting the results from Part I and from the present paper together allows us to account for all the considered sources of disorder in the yarn and in the distortions of the test setup within a single computational model. With the stochastic simulation framework at hand we now proceed with the simulation of the tensile test on yarns and filaments with varied length in order to quantify the significance of the included sources of randomness in a real material.

5.1. Testing of single filament

The most natural way of identifying the distributions of the filament strength and stiffness is to test single filaments with varied length. These experiments have been performed by carefully extracting single filaments from the AR-glass 2400 tex yarns on the testing machine (Fafegraph ME).

However, the tensile test on AR-glass filament has turned out infeasible as far as the measured strength was concerned. The problem was that the measured maximum forces were obviously distorted due to the damage of the glass in the clamps as documented by the big portion of specimens that broke in the vicinity of the clamps. As a result, lower strength has been measured than actually available.

Nevertheless, some information could be extracted from the test results since the positions of break (either free length, or clamp) have been recorded for all specimens. Surprisingly enough, no size effect could be observed on the filaments that broke in the free length on all tested lengths $l = 0.01$, 0.018, 0.030, 0.055, 0.10 m. The explanation for this has been delivered later by the simulations of the bundle tests. As documented further, all the tested filaments fall into the range $l < l_\rho$ (see Fig. 10) with negligible fluctuations of strength and, consequently, without significant size effect.

Fortunately, the measurement of stiffness provided reliable data, especially thanks to the careful documentation of the association between the specimens and the measured response and also of the original positioning of specimens along the filament. Due to the large differences between the filament diameters in the bundle but low fluctuations over its length, it turned out to be very important to quantify the stiffness separately for each group of specimens stemming from the same filament. We appointed the scatter of stiffness solely to E-modulus and quantified the parameters of the distribution $G_E(E)$ as specified in Table 1. The cross-sectional area has been considered constant and has been set to the mean value of diameter determined from the micrographs of the yarn cross-section (see Chudoba et al., 2006, Fig. 6).

Clearly, a good testing of isolated filaments is desirable for its statistical characterization, but the design of a reliable testing set up is by no means trivial. Except of the mentioned distortions, also problems with capturing the influence of coating and of the pre-selection of "better" (stronger) specimens during their extraction from the bundle would have to be addressed.

5.2. Tensile test on a bundle

Because of the difficulties with determining σ using the tensile test on filament, we had to identify the sought distributions with the help of the stochastic simulation of the tests on bundles. Before starting with the calibration procedure we summarize the influence of the individual sources of imperfection on the bundle load strain diagram. For this purpose, we characterize the bundle response by six attributes illustrated in the right figure of Table 2. The signs (+), (−) or (·) denote the positive, negative or neutral tendency in the change of the attributes A-F for increased bundle length. The tendencies are reported for fixed distributions of differences in filament length $l\lambda_{(i)}$, area $A_{(i)}$, activation displacement $l\theta_{(i)}$, strength (given by m, $s_{\xi}f(l)$) and E-modulus.

For example, the first row indicates that the observed evolution of stiffness in the beginning of loading is affected only by filament slack and that it diminishes for longer specimens (because we keep the slack length constant). As a consequence, this effect can be considered in an isolated way and the distribution of slack $G_\theta(\theta)$ can be calibrated separately from the other parameters as it has been done in the companion paper (Chudoba et al., 2006). The identification of $G(\theta)$ has been performed for the average evolution of initial stiffness, see Fig. 15 of Part I.

For the sake of simplicity, θ has not been randomized for each filament. Instead of this, the slack has been assigned to the filaments deterministically following the slack density $G_\theta(\theta)$ in each bundle realization equally. In this way, only the mean load–strain curve gets reproduced with no scatter in the initial part of the curve (attribute A in Table 2). This little methodological transgression resulted in slightly reduced scatter of peak load as can be seen in Fig. 9. In addition, the reduced scatter of peak load can partly be appointed to constant A used in simulations. Nevertheless, neither of these simplifications affects the mean load–strain diagrams. The results of the simulation in comparison with experiments are shown in Fig. 9 without and with the delayed activation. Both filament tensile strength σ and E-modulus were represented by Weibull distributed random process with the autocorrelation structure given in Eq. (6). These two properties were assumed mutually independent and independency was assumed also among filaments. The parameters of distributions of E and σ found to best fit the experiments are listed in the middle columns of Table 1. Following the conclusions from Part I the remaining parameters have not been randomized: λ could be neglected and A has been set constant along and across the bundle. Thus, the identification procedure has been performed for three distributions of the most significant properties: $G_\sigma(\sigma)$ and $G_E(E)$ with the corresponding autocorrelation length and $G_\theta(\theta)$.

The correspondence between the size effect curves obtained in previous sections and the complex size effect observed in the tensile test is shown in Fig. 10. The experimental curve has been reproduced by the stochastic model including the influence of all three random properties simultaneously: E, σ and θ. In order to show the influence of randomness of each parameter separately, the size effect curves have been plotted for isolated randomizations of (θ), (σ) and (σ,E).

In addition to the size effect curves obtained from the random process simulations, Fig. 10 also shows the size effect obtained with the Daniels's and Smith's models calculated for $n = 1600$. Assuming that the filaments follow the Weibull scaling we may construct the bundle power law as a product of Daniels's prediction of the mean total strength specified in Eq. (17) with the Weibull scaling $f(l) = (l_0/l)^{1/m}$

$$\mu^*_{\sigma,l} = \mu^*_\sigma f(l) = \mu^*_\sigma \left(\frac{l_0}{l}\right)^{1/m} = s_0 \cdot m^{-1/m} \cdot \exp(-1/m) \left(\frac{l_0}{l}\right)^{1/m}. \tag{27}$$

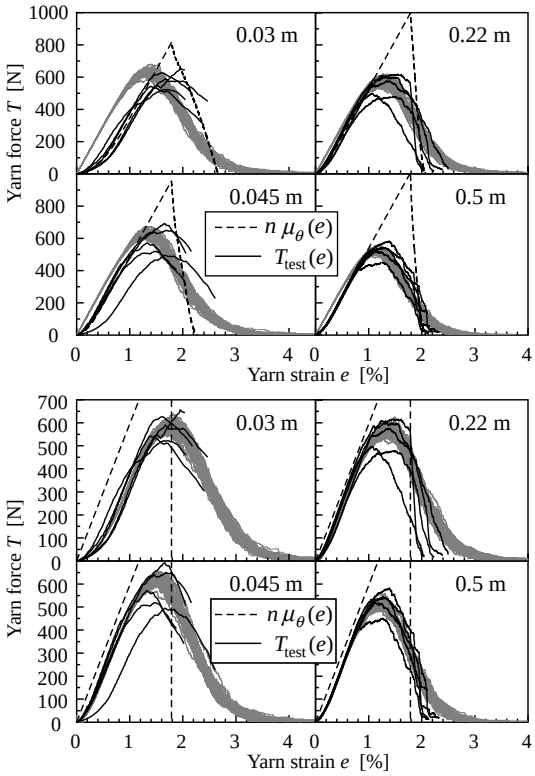

Fig. 9. Comparison of numerical simulations with experiments. Top: simulations with randomized E-modulus and strength σ, without slack. Diagram computed with slack are plotted with dashed line. Bottom: simulations with included delayed activation, randomized E-modulus and strength σ. Diagrams of a perfect yarn $M_0(e)$ are plotted with dashed line.

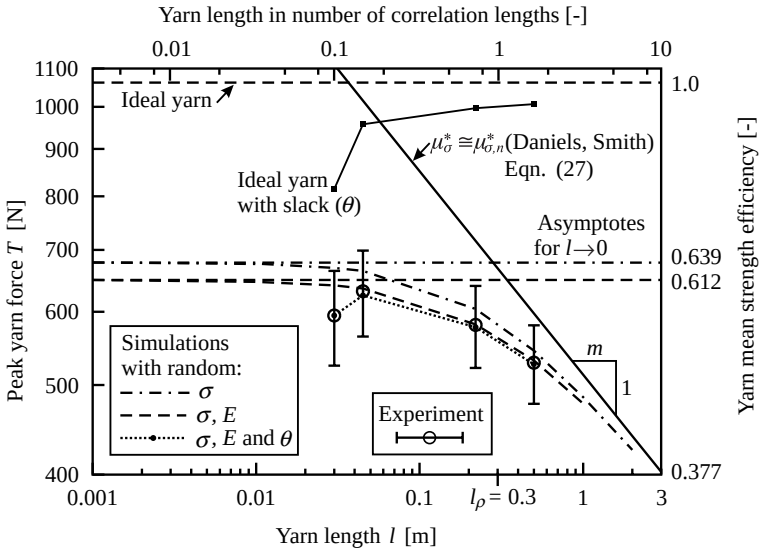

Fig. 10. Mean size effect curves obtained numerically for the randomized σ, θ, σ together with E and all three parameters simultaneously.

The values l_0 and s_0 represent the reference length and scale parameter on the Weibull size-effect line for one filament. The obtained Weibull modulus $m = 4.54$ matches with the size effect measured and calculated for long specimens ($l \gg l_\rho$). We remark, that this value of m falls into the realistic range $m \in \langle 4\text{–}6 \rangle$ for glass fibers.

Regarding the short specimens, the measured total bundle strength departs significantly from the Weibull-type power law (Eq. (27)). This fits into our arguments presented in Section 3 concerning the existence of the statistical length-scale (autocorrelation structure) of the bundle. The computation with random strength and stiffness according to Table 1 (no delayed activation) produces constant size effect for short specimens.

It remains to address the reduction of the total strength observed in the experiment for short specimens (30 mm). As discussed earlier, this reduction may be caused either by the scatter of material stiffness $G_E(E)$ or by the delayed activation $G_\theta(\theta)$. The calculation with these distributions shows that we are able to reproduce the reduction of the total strength measured experimentally. Moreover, the contributions to the strength reduction may be quantified separately for the scatter of E and θ. The reduction of the mean bundle strength due to the scatter of material stiffness remains constant for short specimens $l \ll l_\rho$. Its contribution has been quantified for the performed tests as high as $k_{\sigma,E} = 0.957$ (see Eq. (26)). The reduction due to delayed activation gets intensified for short specimens. In other words, the disorder in the yarn structure dominates the strength reduction for very short specimens.

5.3. Systematic identification of the distribution parameters

Based on the experience with fitting the performed tests we are able to suggest a systematic approach for deriving the statistical characteristics of the multi-filament yarn. The previously described procedure represents the most difficult case including the delayed activation and may be simplified for other types of yarns for which this effect is less pronounced (e.g. polypropylene yarns).

The crucial problem in planning the experimental sequence for constructing the size effect curve is the estimation of the autocorrelation length l_ρ. A possible strategy to estimate the right asymptote of the size effect law is to perform replicated tests on at least two selected lengths $l \gg l_\rho$ and to determine the slope $(-1/m_{\text{slope}})$ of the line connecting the obtained mean strength values in double logarithmic plot as an estimate of the right asymptote of the MSEC.

The determination of the left asymptote requires the test of short bundles $l \ll l_\rho$ usually exhibiting a high amount of experimental distortions (irregular load transmission from the clamps to the filaments). Due to these difficulties it is more effective to test individual filaments extracted from the yarn. The statistical data analysis allows us to determine the Weibull modulus m_{scatter} from Eq. (4). We recommend to test the filaments for at least two lengths in order to ensure that the condition $l \ll l_\rho$ applies for both, i.e. that the estimate of l_ρ is realistic and the mean strength of both lengths is equal. Of course, the moduli m_{scatter} obtained for the two lengths must be identical.

Now, the condition $m_{\text{slope}} = m_{\text{scatter}}$ may be used to verify that the two bundle lengths used to determine the slope of the right asymptote fulfill the condition $l \gg l_\rho$. If $m_{\text{slope}} > m_{\text{scatter}}$, the autocorrelation length l_ρ has probably been underestimated and the chosen specimen lengths are in range $l \approx l_\rho$. In such a case, longer specimens must be tested.

The mean strength measured on filaments (with $l \ll l_\rho$) may be easily transferred to the mean bundle strength with n filaments using the Daniels's or Smith's formulas (17), (18) representing the left asymptote of μ^*_σ. Besides of determining the mean strength, the tests on single filaments can further be exploited to determine the randomness of the E-modulus. The reduction of strength $k_{\sigma,E}$ is performed using Eq. (26).

Finally, the sought autocorrelation length can be determined as an intersection of the two independently determined asymptotes. With the known l_ρ at hand we may express the resulting approximation of the MSEC by Eq. (24).

If the filament strength cannot be measured reliably using filament test as in the case of the used glass filaments (see discussion in Section 5.1) and there is no chance to judge about the autocorrelation length, we have to fit the formula (24) to the data by applying the stochastic simulation of the bundle and find all the parameters of the MSEC by fitting as shown in the previous section.

6. Conclusions

In the two companion papers we have identified and studied several sources of imperfections in the bundle and in the tensile test: delayed activation of filaments, variable cross-sectional area of filaments, scatter of filament clamp distances, variability of E-modulus and of tensile strength along the filaments.

Based on the efficient micromechanical model of the fiber bundle developed in Part I, we have performed stochastic simulations with randomized stiffness and strength along the filaments in the bundle. The size effect formulas derived for studied sources of randomness and their combinations have been verified numerically using a micromechanical model combined with Monte Carlo simulation technique. Based on the lessons learned from the modeling we have suggested approximation formulas describing the size effect laws due to the random strength or stiffness along the bundle. The obtained results have been related to available fiber bundle models and analytical formulas by Daniels, Phoenix and Smith.

An extensive testing program has been worked out so that the results of the simulation could be compared with the test results of the tensile test on bundles and on filaments with varied length. The detailed knowledge of the length-dependent performance of the yarn allowed us to quantify the parameters of statistical distributions of filament and bundle properties stemming from the imperfections in the material structure.

The performed stochastic simulations with the available experimental data revealed the existence of statistical length scale that could be captured by introducing autocorrelation of random material properties. This represents the departure from the classical Weibull-based models that are lacking any kind of length-scale.

The introduced model delivers a quasi-ductile response of the bundle from the ensemble of interacting linear-elastic brittle components with irregular properties. In this respect the present approach falls into the category of lattice models used to model quasi-brittle behavior of concrete. It should be noted, that due to the possibility to trace the failure process in a detailed way both in the experiment and in the simulation, the modeling of multi-filament yarns provides a unique opportunity to study the local effects in quasi-brittle materials. To possibility to generalize the results for other quasi-brittle materials is worth further intensive studies.

The model is limited to bundles with zero friction between filaments. This assumption is justified by the practical focus of the study. In reality, local interaction between filaments would emerge in any yarn with the specimen length sufficiently large with respect to the stress transfer length, i.e. the length at which the equality of local strains gets recovered due to friction. Then, the single bundle gets transformed to a chain of shorter bundles. A systematic study of the transition between the bundle and chain of bundles in combination with other effects studied here is desirable but would go beyond the scope of the present paper.

The obtained statistical material characteristics turned out to be of crucial importance for robust modeling of crack bridges occurring in the cementitious textile composites. The ''well designed'' microstructure of the yarn and of the bond layer in the crack bridge may significantly increase the overall deformation capacity (ductility) of structural elements. The lessons learned from the present study can be applied in a more targeted development of new yarn and textile structures with an improved performance of crack bridges.

As a final remark, we note that the phenomena of delayed activation and varying effective length at the microlevel could be present in any material structure. The only question is at which length scale of material

structure it appears. In case of multi-filament yarns the length scale of delayed activation overlaps with the length scale of other sources of randomness (varying strength and stiffness) so that it must be included in the evaluation of the true size effect.

Acknowledgements

The work has been supported by the German Science Foundation (DFG grant no. ME 725/8-1). The work of the first author has been partially supported by the Ministry of Education of the Czech Republic under the project number 1K-04-110. The support is gratefully acknowledged.

References

Bažant, Z.P., Novák, D., 2000. Probabilistic nonlocal theory for quasi-brittle fracture initiation and size effect. I: Theory. Journal of Engineering Mechanics 126 (2).

Bažant, Z.P., Pang, S.D., Vořechovský, M., Novák, D., Pukl, R., 2004. Statistical size effect in quasibrittle materials: computation and extreme value theory. In: Li, V.C., Willam, K.J., Leung, C.K.Y., Billington, S.L. (Eds.), 5th International Conference FraMCoS—Fracture Mechanics of Concrete and Concrete Structures, vol. 1, Ia-FraMCos, Vail, Colorado, USA, pp. 189–196.

Bažant, Z.P., Planas, J., 1998. Fracture and Size Effect in Concrete and other Quasibrittle Materials. CRC Press, Boca Raton and London.

Bažant, Z.P., Vořechovský, M., Novák, D., 2005. Asymptotic prediction of energetic-statistical size effect from deterministic finite element solutions. Journal of Engineering Mechanics, page in review.

Bažant, Z.P., Xi, Y., 1991. Statistical size effect in quasibrittle structures. II. Nonlocal theory. Journal of Engineering Mechanics 117 (11), 2623–2640.

Castillo, E., 1988. Extreme Value Theory in Engineering. Academic Press, Inc. (London) Ltd.

Chudoba, R., Vořechovský, M., Konrad, M., 2006. Stochastic modeling of multi-filament yarns. I: Random properties within the cross-section and size effect. International Journal of Solids and Structures 43, 412–434.

Daniels, H.E., 1945. The statistical theory of the strength of bundles of threads. Proceedings of the Royal Society (London) 183A, 405.

Daniels, H.E., 1989. The maximum of a Gaussian process whose mean path has a maximum, with an application to the strength of bundles of fibres. Advances of Applied Probability 21, 315–333.

Epstein, B., 1948. Statistical aspects of fracture problems. Journal of Applied Physics 19, 140–147.

Fisher, R.A., Tippett, L.H.C., 1928. Limiting forms of the frequency distribution of the largest and smallest member of a sample. Proceedings of the Cambridge Philosophical Society 24, 180–190.

Gnedenko, B.V., 1943. Sur la distribution limite du terme maximum d'une série aléatorie. Annals of Mathematics, 2nd Series 44 (3), 423–453.

Gumbel, E.J., 1958. Statistics of Extremes. Columbia University Press, New York.

Hohenbichler, M., 1983. Resistance of large brittle parallel systems. In: ICASP 4, International Conference on Applications of Statistics and Probability in Soil and Structural Engineering, University of Firenze, Italy, pp. 1301–1312.

Hohenbichler, M., Rackwitz, R., 1983. Reliability of parallel systems under imposed uniform strain. Journal of Engineering Mechanics 109 (3), 896–907.

Iman, R., Conover, W., 1980. Small sample sensitivity analysis techniques for computer models with an application to risk assessment. Communications in Statistics: Theory and Methods A9 (17), 1749–1842.

Iman, R., Conover, W., 1982. A distribution free approach to inducing rank correlation among input variables. Communications in Statistics B11, 311–334.

Novák, D., Lawanwisut, W., Bucher, C., 2000. Simulation of random fields based on orthogonal transformation of covariance matrix and Latin Hypercube Samplings. In: Schuëller, G.I., Spanos, P.D. (Eds.), International Conference on Monte Carlo Simulation (MCS 2000). Swets & Zeitlinger, Lisse (2001). Monaco, Monte Carlo, pp. 129–136.

Olsson, J., Sandberg, G., 2002. Latin hypercube sampling for stochastic finite element analysis. Journal of Engineering Mechanics 128 (1), 121–125, Technical Note.

Phoenix, S.L., 1974. Probabilistic strength analysis of fibre bundle structures. Fibre Sciences and Technology 7, 15–31.

Phoenix, S.L., 1975. Probabilistic inter-fiber dependence and the asymptotic strength distribution of classic fiber bundles. International Journal of Engineering Science 13, 287–304.

Phoenix, S.L., 1979. Statistical theory for the strength of twisted fiber bundles with applications to yarns and cables. Textile Research Journal, 407–423.

Phoenix, S.L., Taylor, H.M., 1973. The asymptotic strength distribution of a general fiber bundle. Advances in Applied Probability 5, 200–216.

Smith, R.L., 1982. The asymptotic distribution of a series-parallel system with equal load-sharing. The Annals of Probability 10 (1), 137–171.

Vořechovský, M., 2004. Stabilita a konvergence numerických metod při simulaci extrémních hodnot rozdělení (Stability and convergence of numerical methods for simulation of statistics of extremes). In: PPK 2004 Pravděpodobnost porušování konstrukcí. Brno University of Technology, Brno, Czech Republic, pp. 257–264 (in Czech).

Vořechovský, M., in preparation. Comparison of stability and accuracy of numerical simulation methods for simulation of statistics of extremes. Probabilistic Engineering Mechanics.

Vořechovský, M., submitted for publication. Simulation of cross-correlated random fields by series expansion methods. Structural Safety.

Vořechovský, M., Novák, D., 2002. Correlated random variables in probabilistic simulation. In: Schießl, P., Gebbeken, N., Keuser, M., Zilch, K. (Eds.), 4th International Ph.D. Symposium in Civil Engineering, Munich, Germany. Millpress, Rotterdam, pp. 410–417.

Vořechovský, M., Novák, D., 2003. Efficient random fields simulation for stochastic fem analyses. In: Der Kiureghian, M.P. (Ed.), 2nd M.I.T. Conference on Computational Fluid and Solid Mechanics, Cambridge, USA. Millpress, Rotterdam, pp. 2383–2386.

Weibull, W., 1939The Phenomenon of Rupture in Solids, vol. 153. Royal Swedish Institute of Engineering Research (Ingenioersvetenskaps Akad. Handl.), Stockholm, 1–55.